Animal venoms …

… represent a rich source of pharmacologically active peptides that interact with ion channels. In their Communication on page 9306 ff., H. Zhang, R. A. Lerner et al. describe an autocrine-based method to select functional venom peptides from their vast repertoire in nature. This method allows about 100 million different venoms to be studied in a single experiment, and its utility was demonstrated by the discovery of novel Kv1.3 channel blockers from a natural venom peptide library.

Redox Chemistry

In their Communication on page 9168 ff., X. Lu, H.-C. Xu et al. describe the efficient electrochemical synthesis of highly functionalized indoles and azaindoles. Ferrocene is used as the redox catalyst, and the only theoretical byproduct is H_2.

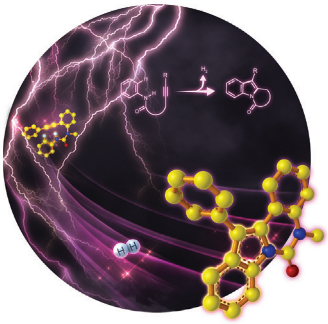

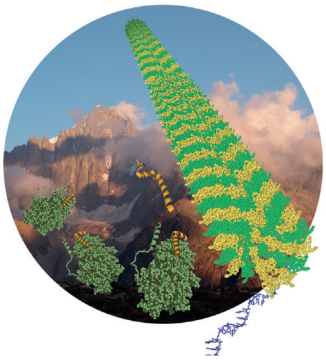

Capsid Self-Assembly

In their Communication on page 9356 ff., R. W. H. Ruigrok, M. Blackledge et al. discuss the self-organization of recombinant nucleoproteins into long nucleocapsid-like helices, simply upon addition of RNA.

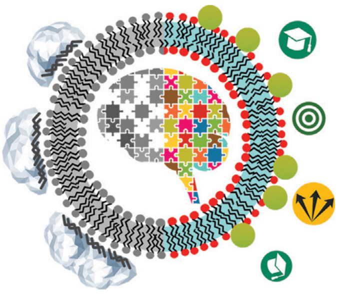

Alzheimer's Disease

The oligomerization of β-amyloid is thought to spark Alzheimer's disease. Insights into the roles of sphingomyelin and GM_1 ganglioside in this process are described by M. Amaro, M. Hof et al. in their Communication on page 9411 ff.

How to contact us:

Editorial Office:
E-mail: angewandte@wiley-vch.de
Fax: (+49) 6201–606-331
Telephone: (+49) 6201–606-315

Reprints, E-Prints, Posters, Calendars:
Carmen Leitner
E-mail: chem-reprints@wiley-vch.de
Fax: (+49) 6201–606-331
Telephone: (+49) 6201–606-327

Copyright Permission:
Bettina Loycke
E-mail: rights-and-licences@wiley-vch.de
Fax: (+49) 6201–606-332
Telephone: (+49) 6201–606-280

Online Open:
Margitta Schmitt
E-mail: angewandte@wiley-vch.de
Fax: (+49) 6201–606-331
Telephone: (+49) 6201–606-315

Subscriptions:
www.wileycustomerhelp.com
Fax: (+49) 6201–606-184
Telephone: 0800 1800536 (Germany only)
+44(0) 1865476721 (all other countries)

Advertising:
Marion Schulz
E-mail: mschulz@wiley-vch.de
Fax: (+49) 6201–606-550
Telephone: (+49) 6201–606-565

Courier Services:
Boschstrasse 12, 69469 Weinheim

Regular Mail:
Postfach 101161, 69451 Weinheim

Angewandte Chemie International Edition is a journal of the Gesellschaft Deutscher Chemiker (GDCh), the largest chemistry-related scientific society in continental Europe. Information on the various activities and services of the GDCh, for example, cheaper subscription to *Angewandte Chemie International Edition*, as well as applications for membership can be found at **www.gdch.de** or can be requested from GDCh, Postfach 900440, D-60444 Frankfurt am Main, Germany.

GESELLSCHAFT DEUTSCHER CHEMIKER

© 2016 Wiley-VCH Verlag GmbH & Co. KGaA, Weinheim

Get the Angewandte App
International Edition

ANDROID APP ON Google Play

Available on the App Store

Enjoy Easy Browsing and a New Reading Experience on Your Smartphone or Tablet
- Keep up to date with the latest articles in Early View.
- Download new weekly issues automatically when they are published.
- Read new or favorite articles anytime, anywhere.

Editorial

“ ... The number of universities teaching nuclear and radiochemistry has decreased, not least as radiochemistry is erroneously linked to the use of nuclear power ... Radiochemistry is essential for a variety of fields, including radiopharmaceuticals, as well as the management of radioactive waste ... we are facing a lack of specialists in the area of radiation protection ...”
Read more in the Editorial by Clemens Walther.

Service

Author Profile

“When I was eighteen I wanted to be an architect. Chemistry is fun because it is absolutely unpredictable ...”
This and more about Bernd Plietker can be found on page 9128.

News


D. Segets


S. Kobayashi


T. Carell


A. G. Beck-Sickinger


E. Hey-Hawkins

Highlights

Computational Chemistry

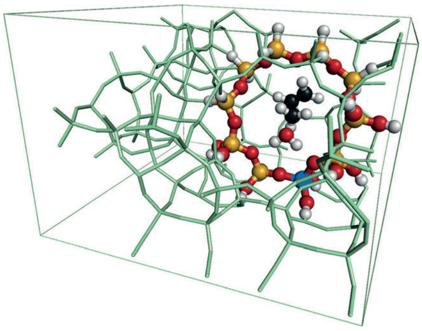

Ex machina: A computational method for predicting rate constants for reactions within microporous zeolite catalysts with chemical accuracy has recently been reported. A key feature of this method is a stepwise QM/MM approach that allows accuracy to be achieved while using realistic models with accessible computer resources.

Reviews

Metal Carbenes

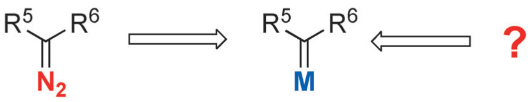

Metal carbenes without diazo compounds? In the past, diazo compounds were most commonly used for the generation of metal carbenes under metal catalysis. With concerns over safety and large-scale syntheses, many other substrates are now available as surrogates for this purpose, and their applications are summarized in this Review.

For the USA and Canada:
ANGEWANDTE CHEMIE International Edition (ISSN 1433-7851) is published weekly by Wiley-VCH, PO Box 101161, 69451 Weinheim, Germany. US mailing agent: SPP, PO Box 437, Emigsville, PA 17318. Periodicals postage paid at Emigsville, PA. US POSTMASTER: send address changes to *Angewandte Chemie*, John Wiley & Sons Inc., C/O The Sheridan Press, PO Box 465, Hanover, PA 17331. Annual subscription price for institutions: US$ 16.862/14.051 (valid for print and electronic / print or electronic delivery); for individuals who are personal members of a national chemical society prices are available on request. Postage and handling charges included. All prices are subject to local VAT/sales tax.

© 2016 Wiley-VCH Verlag GmbH & Co. KGaA, Weinheim

Communications

Redox Chemistry

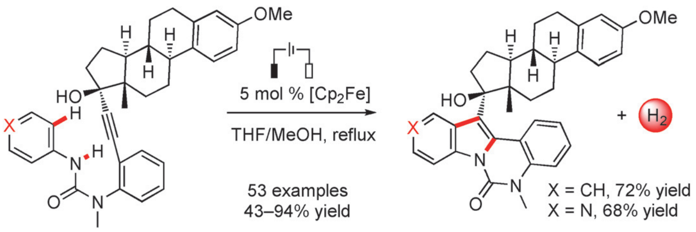

It's electric: An electrochemical coupling of (hetero)arylamines with tethered alkynes has been developed and provides highly chemo- and regioselective access to densely functionalized indoles and azaindoles. The electrochemical reaction employs ferrocene ([Cp$_2$Fe]), an inexpensive organometallic reagent, as the redox catalyst and produces H$_2$ as the only theoretical byproduct.

Z.-W. Hou, Z.-Y. Mao, H.-B. Zhao, Y. Y. Melcamu, X. Lu,* J. Song, H.-C. Xu* ______ **9168 – 9172**

Electrochemical C−H/N−H Functionalization for the Synthesis of Highly Functionalized (Aza)indoles

Frontispiece

Sustainable Chemistry

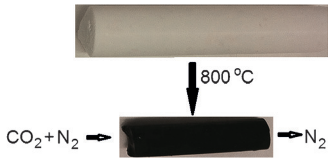

The impact of mesoporosity: Mesoporous carbon materials (Starbons®) derived from waste biomass show an enhanced carbon dioxide capture capacity and an enhanced selectivity for carbon dioxide compared to microporous activated carbon. This effect is due to the presence of micropore–mesopore interfaces.

G. Durá, V. L. Budarin, J. A. Castro-Osma, P. S. Shuttleworth, S. C. Z. Quek, J. H. Clark,* M. North* ______ **9173 – 9177**

Importance of Micropore–Mesopore Interfaces in Carbon Dioxide Capture by Carbon-Based Materials

---

Shape-Selective Catalysis

Shape-selective reactions over a palladium nanoparticle (Pd NP) based catalyst were achieved by integrating Pd NPs inside mesoporous silicalite-1 nanocrystals. The unique micro- and mesoporous structure of the zeolite nanocrystals endowed Pd NPs both high stability and excellent shape selectivity for organic synthesis.

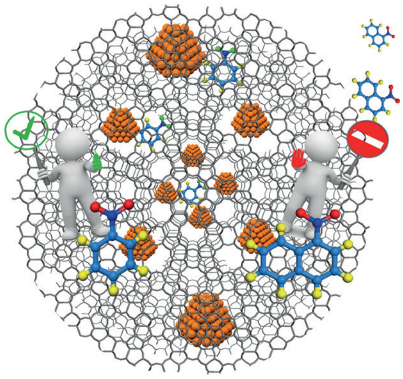

T. L. Cui, W. Y. Ke, W. B. Zhang, H. H. Wang, X. H. Li,* J. S. Chen* ______ **9178 – 9182**

Encapsulating Palladium Nanoparticles Inside Mesoporous MFI Zeolite Nanocrystals for Shape-Selective Catalysis

---

Organocatalysis

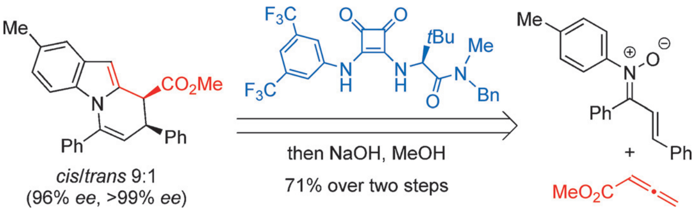

Take your partners, join the dance: Chiral squaramide catalysts promote the asymmetric synthesis of dihydropyridoindoles from simple, non-indole reagents. In this complex cascade process, the catalyst appears to interact with reactive intermediates to control both regio- and enantioselectivity. A subsequent epimerization step increases the diastereomeric ratio of the products, while retaining high enantiomeric purity.

W. H. Pace, D.-L. Mo, T. W. Reidl, D. J. Wink, L. L. Anderson* **9183 – 9186**

Catalytic Asymmetric Synthesis of Dihydropyrido[1,2-*a*]indoles from Nitrones and Allenoates

P_4 Functionalization

L. Xu, Y. Chi, S. Du, W.-X. Zhang,*
Z. Xi ______ **9187 – 9190**

Direct Synthesis of Phospholyl Lithium from White Phosphorus

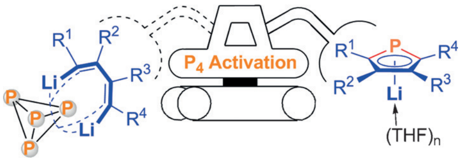

Pull it together: Phospholyl lithium derivatives were synthesized directly from P_4 and 1,4-dilithio-1,3-butadienes with excellent efficiency. DFT calculations indicate that the mechanism of this reaction differs from the well-known stepwise cleavage of P—P bonds in P_4 activation. Instead, a cooperative nucleophilic attack of two C_{sp^2}—Li bonds on P_4 is preferred.

Stretchable Supercapacitors

T. Lv, Y. Yao, N. Li, T. Chen* **9191 – 9195**

Highly Stretchable Supercapacitors Based on Aligned Carbon Nanotube/ Molybdenum Disulfide Composites

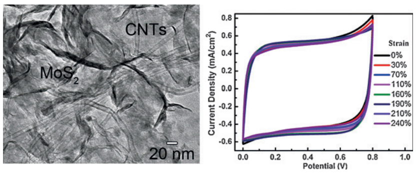

At full stretch: Using highly aligned CNT/ MoS_2 composites, stretchable all-solid-state supercapacitors are prepared that sustain their electrochemical performance after being stretched by 240%. They also exhibited excellent cycling stability after 10000 charge–discharge cycles.

Flexible Supercapacitors

W. Li, F. Gao, X. Wang, N. Zhang,
M. Ma* ______ **9196 – 9201**

Strong and Robust Polyaniline-Based Supramolecular Hydrogels for Flexible Supercapacitors

For whom the gel toils: Inspired by the dynamic network structure of animal dermis, a strong and robust conductive hydrogel is prepared by supramolecular assembly of polyaniline and polyvinyl alcohol. Flexible solid-state supercapacitors based on the hydrogel show excellent capacitance and energy density and outstanding mechanical robustness.

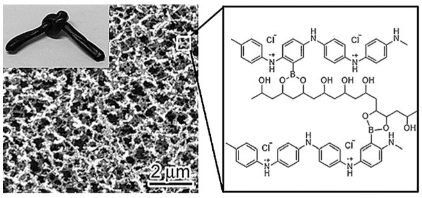

Polymers

C. Yang, B. C. Ma, L. Zhang, S. Lin,
S. Ghasimi, K. Landfester, K. A. I. Zhang,*
X. Wang* ______ **9202 – 9206**

Molecular Engineering of Conjugated Polybenzothiadiazoles for Enhanced Hydrogen Production by Photosynthesis

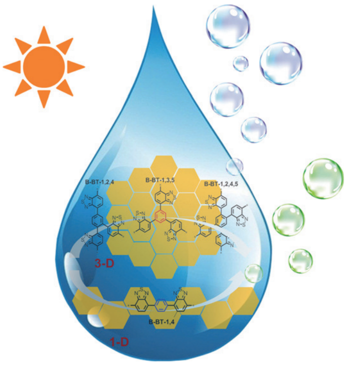

Bring to light: Conjugated polybenzothiadiazoles were introduced as a new family of organic photocatalysts for H_2 evolution from water in the presence of electron donors with visible-light irradiation. The molecular engineering of the electron-withdrawing benzothiadiazole unit on the phenyl unit allows the construction of either one- or three-dimensional polybenzothiadiazoles, and the effect of the structure on the photocatalytic H_2 evolution activity was investigated.

© 2016 Wiley-VCH Verlag GmbH & Co. KGaA, Weinheim

Hydrogenation

T. Liang, S. K. Woo,
M. J. Krische* ____ **9207 – 9211**

C-Propargylation Overrides O-Propargylation in Reactions of Propargyl Chloride with Primary Alcohols: Rhodium-Catalyzed Transfer Hydrogenation

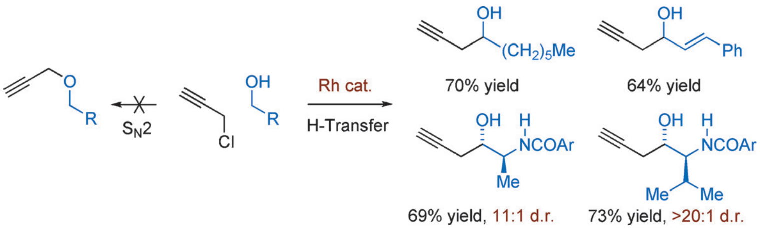

A path less travelled: The canonical S_N2 behavior displayed by alcohols and activated alkyl halides in basic media (O-alkylation) is superseded by a pathway leading to carbinol C-alkylation under the conditions of rhodium-catalyzed transfer hydrogenation. Racemic and asymmetric propargylations are described.

Porphyrinoids

Y. Okuda, E. Tsurumaki, J. Oh, J. Sung,
D. Kim,* A. Osuka* ____ **9212 – 9215**

A Directly Fused Subporphyrin Dimer with a Wavelike Structure

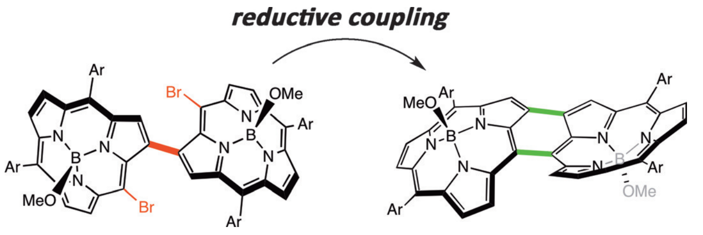

Link up: $[Ni(cod)_2]$-mediated intramolecular reductive coupling of a β–β′ linked meso,meso′-dibromosubporphyrin dimer gave the *anti*-isomer of a fused subporphyrin dimer. The new dimer displays a wavelike coplanar structure, a perturbed and red-shifted absorption spectrum, reversible redox behaviors with a decreased electrochemical HOMO–LUMO band gap, and a shortened S_1-state lifetime owing to the effective conjugation through fusion.

Frustrated Lewis Pairs

K.-Y. Ye, G. Kehr, C. G. Daniliuc, L. Liu,
S. Grimme, G. Erker* ____ **9216 – 9219**

Coupling of Carbon Monoxide with Nitrogen Monoxide at a Frustrated Lewis Pair Template

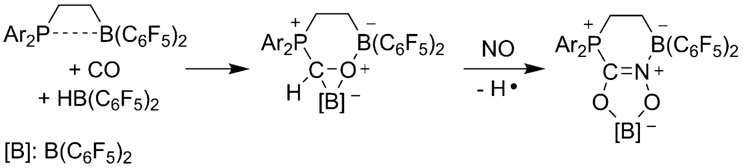

Couples and pairs: Coupling of carbon monoxide with nitrogen monoxide was achieved at a frustrated Lewis pair template. This unique reaction uses hydride as an auxiliary, which reductively activates carbon monoxide at the frustrated Lewis pair. The CO/NO coupling reaction then takes place through a pathway involving a radical reaction in which the hydrogen atom auxiliary is eventually removed again.

Cycloaddition

Q.-J. Liu, L. Wang, Q.-K. Kang,
X. P. Zhang,* Y. Tang* ____ **9220 – 9223**

Cy-SaBOX/Copper(II)-Catalyzed Highly Diastereo- and Enantioselective Synthesis of Bicyclic N,O Acetals

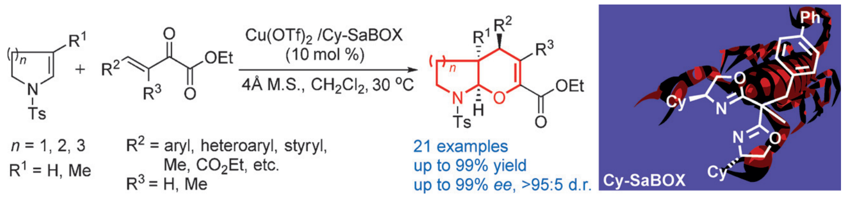

N,O skeletons: A protocol for the enantioselective construction of useful and important bicyclic N,O-acetal skeletons is described. Excellent yields and excellent stereoselectivities were obtained for a broad scope of substrates, and even with only a 1 mol% catalyst loading on gram scale.

Polycycle Synthesis

J. Zhu, Y.-J. Cheng, X.-K. Kuang, L. Wang,* Z.-B. Zheng, Y. Tang* ——— **9224 – 9228**

Highly Efficient Formal [2+2+2] Strategy for the Rapid Construction of Polycyclic Spiroindolines: A Concise Synthesis of 11-Demethoxy-16-*epi*-myrtoidine

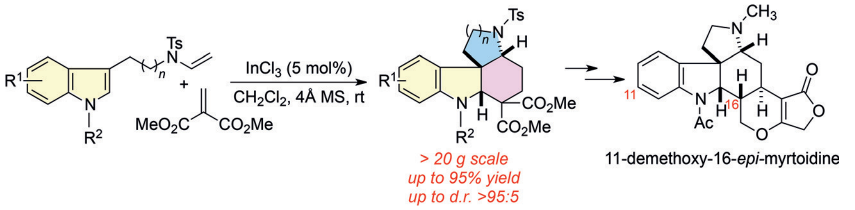

Going full cycle: Upon treatment with the catalyst $InCl_3$ (5 mol %), tryptamine-derived enamides reacted readily with methylene malonate to provide rapid, gram-scale access to versatile tetracyclic spiroindolines with excellent diastereoselectivity (see scheme). This strategy offers a concise approach to alkaloids isolated from *Strychnos myrtoides*, as demonstrated by a short synthesis of 11-demethoxy-16-*epi*-myrtoidine.

Water Splitting

W. Y. Wang, H. Wang, Q. J. Zhu, W. Qin, G. Y. Han, J. Shen, X. Zong,* C. Li* ——— **9229 – 9233**

Spatially Separated Photosystem II and a Silicon Photoelectrochemical Cell for Overall Water Splitting: A Natural–Artificial Photosynthetic Hybrid

A hybrid natural–artificial photosynthetic platform was constructed by wiring photosystem II and a silicon photoelectrochemical cell based on a photocatalytic–photoelectrochemical Z-scheme design. The hybrid platform combined the strengths of natural and artificial platforms and achieved unassisted and spatially separated production of H_2 and O_2 from water splitting under solar irradiation.

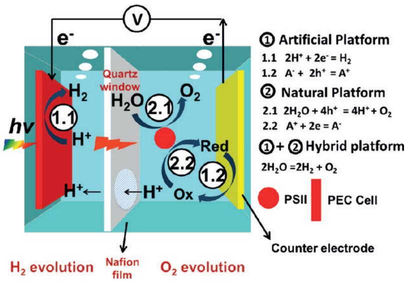

Metallofullerenes

L. Bao, C. Pan, Z. Slanina, F. Uhlik, T. Akasaka, X. Lu* ——— **9234 – 9238**

Isolation and Crystallographic Characterization of the Labile Isomer of $Y@C_{82}$ Cocrystallized with Ni(OEP): Unprecedented Dimerization of Pristine Metallofullerenes

It takes two: The dimerization of a pristine metallofullerene is observed for the first time in the crystal structure of the labile minor isomer of $Y@C_{82}$, unambiguously assigned as $Y@C_s(6)\text{-}C_{82}$. In contrast, under identical conditions the major isomer $Y@C_{2v}(9)\text{-}C_{82}$ does not form dimers, indicative of a cage-symmetry-induced process which can be rationalized by considering the localization of spin densities on the fullerene cages.

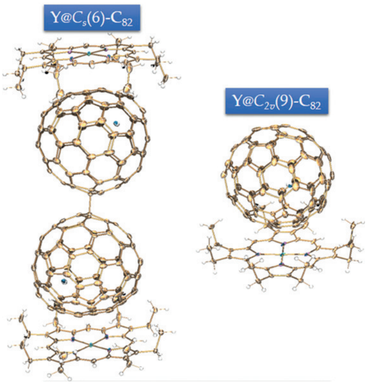

Metal–Metal Bonds

A. J. Boutland, D. Dange, A. Stasch, L. Maron,* C. Jones* ——— **9239 – 9243**

Two-Coordinate Magnesium(I) Dimers Stabilized by Super Bulky Amido Ligands

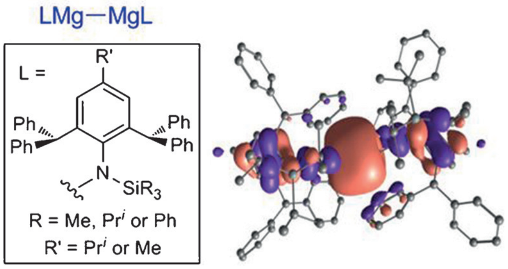

Two's company: Reduction of extremely bulky amido magnesium iodide complexes with KC_8 yields two-coordinate magnesium(I) dimers, LMg–MgL, which crystallographic and DFT computational studies show to possess unsupported Mg–Mg covalent bonds of high s-character. THF adducts of two of these complexes are also reported.

© 2016 Wiley-VCH Verlag GmbH & Co. KGaA, Weinheim

Synthetic Methods

N. J. Green, A. C. Willis,
M. S. Sherburn* ———— 9244 – 9248

Direct Cross-Couplings of Propargylic Diols

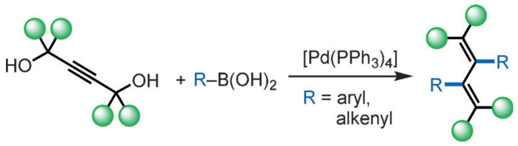

Just diene to form from a diol! Underivatized propargylic diols are now substrates for two-fold Suzuki–Miyaura couplings and deliver a wide range of highly substituted 1,3-dienes in one step. The cross-coupling reaction is likely facilitated by coordination of boron to the hydroxy groups of the diol, and the product can be used to readily generate a number of highly substituted polyenic systems.

Multicomponent Reactions

T. M. Ha, C. Chatalova-Sazepin, Q. Wang,
J. Zhu* ———— 9249 – 9252

Copper-Catalyzed Formal [2+2+1] Heteroannulation of Alkenes, Alkylnitriles, and Water: Method Development and Application to a Total Synthesis of (±)-Sacidumlignan D

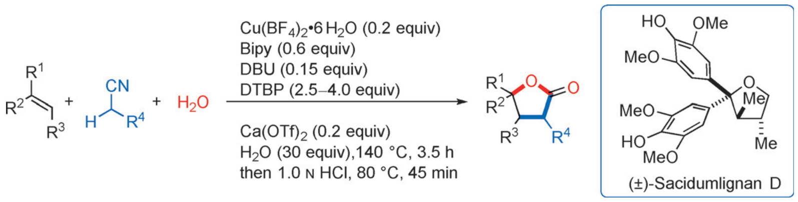

Water connections: The title reaction affords γ-butyrolactones with the creation of three chemical bonds and a quaternary carbon center. The domino process involves an unprecedented copper-catalyzed hydroxy-cyanoalkylation of alkenes. A total synthesis of (±)-sacidumlignan D was accomplished featuring this heteroannulation as a key step.

Platinum Clusters

B. R. Barnett, A. L. Rheingold,
J. S. Figueroa* ———— 9253 – 9258

Monomeric Chini-Type Triplatinum Clusters Featuring Dianionic and Radical-Anionic π*-Systems

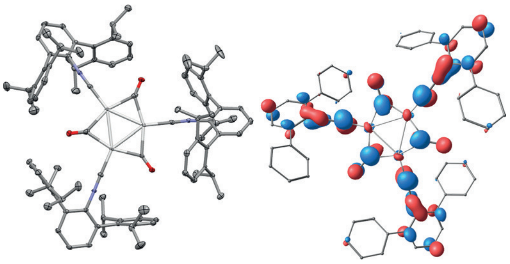

Unstacking the deck: The dianionic "Chini clusters" consist of stacked *triangulo*-$Pt_3(CO)_6$ units, but the parent species $[Pt_3(CO)_6]^{2-}$ has eluded structural characterization. Sterically demanding *m*-terphenyl isocyanides ($CNAr^{Dipp2}$) allow for the isolation of isolobal $K_2[Pt_3(\mu\text{-}CO)_3(CNAr^{Dipp2})_3]$ as well as the corresponding monoanionic radical. The highest occupied orbital in both is primarily CO/CNR π*, which results in ligand-based redox non-innocence.

Weakly Coordinating Anions

P. J. Malinowski, D. Himmel,
I. Krossing* ———— 9259 – 9261

Silver Complexes of Dihalogen Molecules

Catch a dihalogen: The donor-free and coordinatively unsaturated silver compound $Ag[Al(OR^F)_4]$ ($R^F = C(CF_3)_3$) is slightly soluble in perfluorohexane. The compound takes up the simple and weakly basic dihalogen molecules Cl_2, Br_2, and I_2 as ligands.

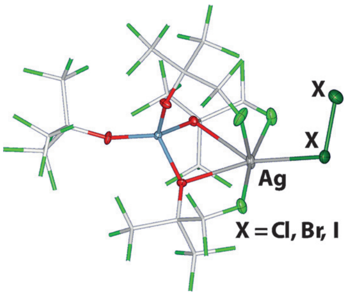

© 2016 Wiley-VCH Verlag GmbH & Co. KGaA, Weinheim

Weakly Coordinating Anions

P. J. Malinowski, D. Himmel,
I. Krossing* ______________ 9262 – 9266

Coordination Chemistry of Diiodine and Implications for the Oxidation Capacity of the Synergistic Ag^+/X_2 ($X = Cl, Br, I$) System

Coordination chemistry of diiodine: Silver(I) ions and diiodine molecules are an unexpectedly variable couple that form dication salts with up to six diiodine molecules as well as the molecule **A**Ag-I$_2$-Ag**A** (**A** = [Al(OR^f)$_4$], R^f = C(CF$_3$)$_3$). This molecule presents an easily in bulk accessible strong oxidizer converting pentane and propane into carbocations, and white phosphorus into P_9^+.

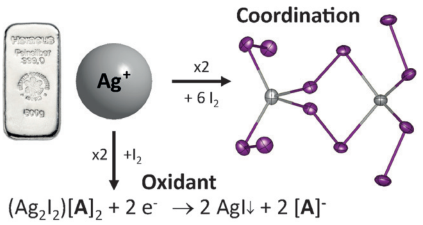

Metal-Oxide Films

L. R. Merte,* C. J. Heard, F. Zhang,
J. Choi, M. Shipilin, J. Gustafson,
J. F. Weaver, H. Grönbeck,
E. Lundgren ______________ 9267 – 9271

Tuning the Reactivity of Ultrathin Oxides: NO Adsorption on Monolayer FeO(111)

Tailored chemisorption: Supported oxide monolayers exhibit novel chemical properties that can be exploited for applications in catalysis. Drastic differences in the adsorption of NO on supported FeO monolayers are observed, depending on the metal substrate. These differences are found to result from steric blocking, which is due to substrate-induced buckling of the FeO films.

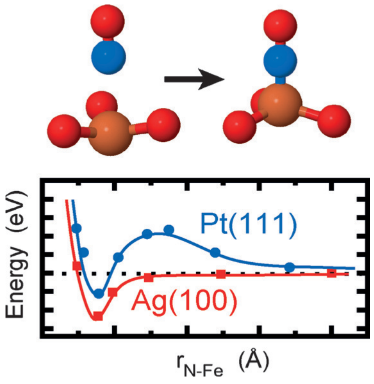

Theranostic Nanoparticles

C. Yu, L. Qian, J. Ge, J. Fu, P. Yuan,
S. C. L. Yao, S. Q. Yao* ______ 9272 – 9276

Cell-Penetrating Poly(disulfide) Assisted Intracellular Delivery of Mesoporous Silica Nanoparticles for Inhibition of miR-21 Function and Detection of Subsequent Therapeutic Effects

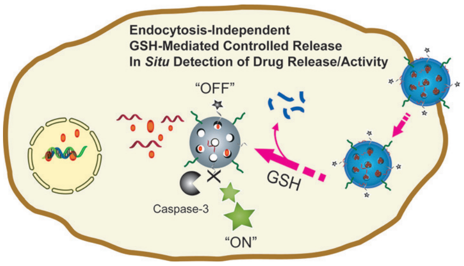

Combine and detect: Mesoporous silica nanoparticles are coated with cell-penetrating poly(disulfide)s and a fluorogenic apoptosis-detecting peptide. The result is a theranostic drug delivery system for endocytosis-independent delivery/controlled release of combination drugs for the inhibition of endogenous miR-21 with simultaneous detection of subsequent drug effects by two-photon fluorescence microscopy.

Structure Elucidation

P. Kahl, J. P. Wagner, C. Balestrieri,
J. Becker, H. Hausmann, G. J. Bodwell,
P. R. Schreiner* ____________ 9277 – 9281

[2](1,3)Adamantano[2](2,7)pyrenophane: A Hydrocarbon with a Large Dipole Moment

Diamond in the rough: Molecular electronics with single hydrocarbons may be possible by combining the sp^3-hybridized diamond with sp^2-hybridized graphene carbon allotropes. This combination is mimicked through the combination of a diamondoid with pyrene as a graphene model. The nonpolar components lead to a new, highly strained hydrocarbon with a very large and optimally positioned dipole moment needed for molecular rectification.

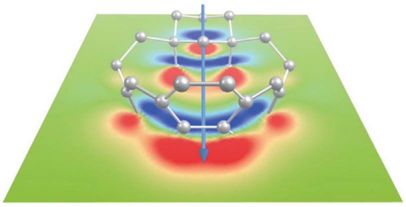

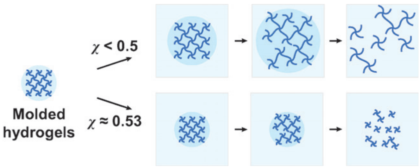

Degradation without swelling: Hydrogels with an optimal polymer–solvent interaction parameter were synthesized to achieve non-osmotic conditions. The resultant non-osmotic hydrogels displayed the capability to retain their original shape (see picture) and degrade without accompanying significant morphological changes under physiological conditions.

Hydrogels

Changing phases: The thermally induced cubic–tetragonal phase transition of an sII clathrate hydrate containing 2-propanol causes volume expansion. This transition is most likely related to the restriction of the motion of 2-propanol within the host water cage.

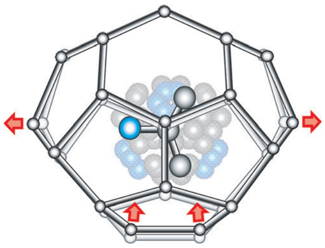

Phase Transitions

Amyloid formation: While deuteration shows no major impact on the transthyretin (TTR) crystal structure, the labeling affects protein kinetics significantly. This behavior is reflected in differing levels of TTR subunit exchange and also in the rate of amyloid formation. Deuteration effects are comparable to effects observed in the case of aggressive TTR.

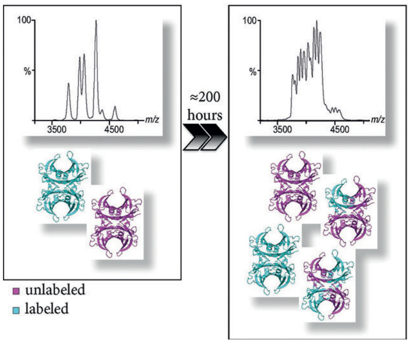

Mass Spectrometry

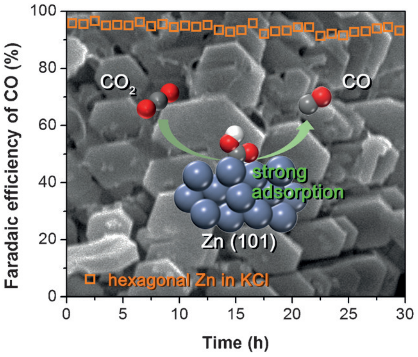

CO_2 conversion: A design strategy for efficient carbon dioxide reduction is suggested using a well-synthesized hierarchical hexagonal Zn catalyst which shows highly selective and, more importantly, stable performance towards carbon monoxide production (see picture). The manipulation of the Zn crystal structure and its facet ratio (101)/(002) can be used as a key control factor for product selectivity.

Electrocatalysis

© 2016 Wiley-VCH Verlag GmbH & Co. KGaA, Weinheim

Plant Glycobiology

Y. Zhu, J. Wu, X. Chen* **9301 – 9305**

Metabolic Labeling and Imaging of N-Linked Glycans in *Arabidopsis Thaliana*

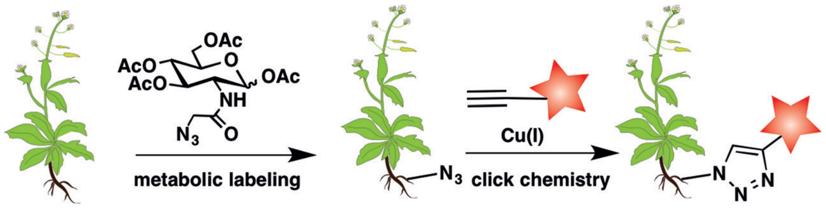

Glycan imaging in plants: N-linked glycosylation is metabolically labeled with an azide-functionalized sugar reporter, which enables click-labeling and fluorescence imaging of N-glycans in *Arabidopsis thaliana*.

Venom Peptides

H. Zhang,* M. Du, J. Xie, X. Liu, J. Sun, W. Wang, X. Xin, L. D. Possani, K. Yea, R. A. Lerner* **9306 – 9310**

Autocrine-Based Selection of Drugs That Target Ion Channels from Combinatorial Venom Peptide Libraries

Front Cover

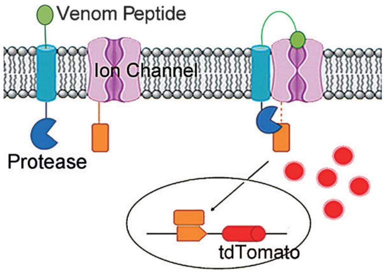

Pick your poison: Cysteine-knot peptides were extracted from the venom database by using bioinformatics and used to create a lentiviral vector library for the autocrine-based selection of peptides targeting ion channels. Interaction of the membrane-tethered venom peptide with the ion channel results in the protease-mediated release of a transcription factor (orange), which triggers expression of a reporter gene (red).

Synthetic Receptors

T. S. Carter, T. J. Mooibroek, P. F. N. Stewart, M. P. Crump, M. C. Galan, A. P. Davis* **9311 – 9315**

Platform Synthetic Lectins for Divalent Carbohydrate Recognition in Water

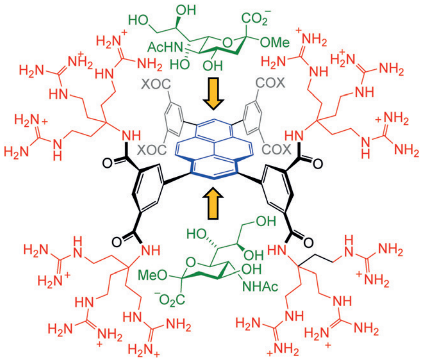

Be my guests: Carbohydrate receptors featuring two equivalent binding sites were designed to target facially amphiphilic substrates. A version with anionic side chains favors aminosugars, whereas a cationic variant binds the biologically important α-sialyl unit (as shown).

Extended Aromatic Structures

S. Dong, T. S. Herng, T. Y. Gopalakrishna, H. Phan, Z. L. Lim, P. Hu, R. D. Webster, J. Ding, C. Chi* **9316 – 9320**

Extended Bis(benzothia)quinodimethanes and Their Dications: From Singlet Diradicaloids to Isoelectronic Structures of Long Acenes

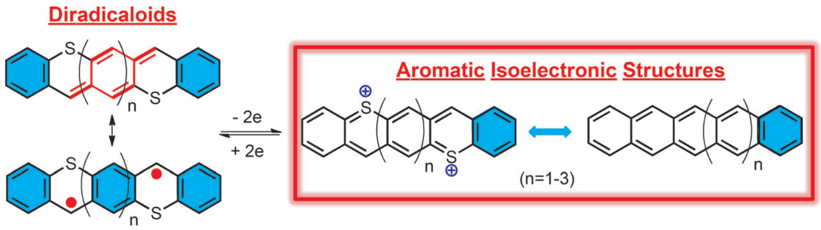

Isoelectronic to acenes: Extended bis(benzothia)quinodimethanes show increased diradical character with increasing molecular length. More importantly, their dications exhibit similar electronic structures to their corresponding all-carbon acene analogues and can be regarded as being genuine isoelectronic analogues of acenes.

© 2016 Wiley-VCH Verlag GmbH & Co. KGaA, Weinheim

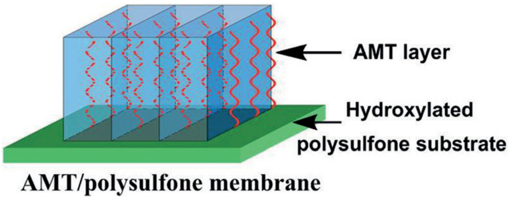

A mixed-matrix membrane consisting of aligned montmorillonite (AMT) and polysulfone was prepared for CO_2 separation. The MT interlayer gaps were aligned with polyvinylamineacid chains that had been grafted onto the surface of the hydroxylated polysulfone substrate. The high-speed transport channels in AMT result in high CO_2 permeance and mixed-gas permselectivity.

Gas Separation

Liquid interfaces: For a full understanding of the ion transfer during solvent extraction, knowledge about the extractant and ion distributions across the water–oil interface is necessary. The extractant and ion distributions at the water–oil interface were studied by X-ray and neutron reflectivity measurements for two different diamide extractants (see picture).

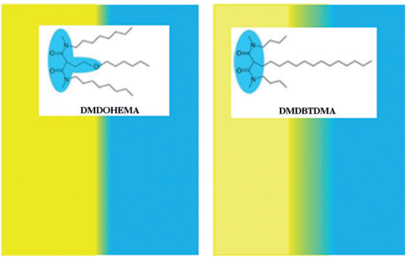

Sustainable Chemistry

Isolated formamide$_2$–water can be taken as a simple model for water-mediated interactions and amide self-association. The structure and the electric field gradient determined at the nitrogen nuclei measured from the rotational spectrum reveal the subtle inductive effects that polarize the amide group and alter the C=O and N–C distances of formamide.

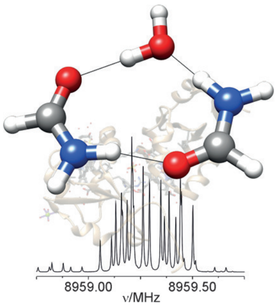

Hydrogen Bonding

Two-faced: A perfect "Janus cube" octasilsesquioxane, a nanoscale Janus particle with two different types of substituents, was synthesized through the cross-coupling of a "half-cube" sodium cyclosiloxanolate with another half-cube cyclic fluorosiloxane. The structure was confirmed by X-ray crystallography to be a Janus cube. Furthermore, this method represents a novel siloxane bond-forming reaction involving the coupling of a silanol salt and fluorosilane.

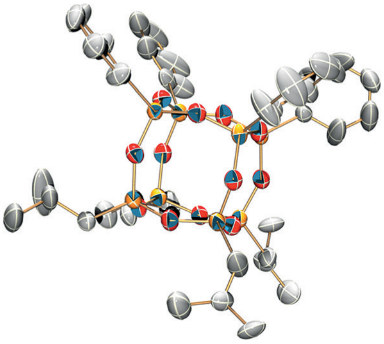

Siloxanes

Double Perovskites

E. Solana-Madruga, Á. M. Arévalo-López,
A. J. Dos Santos-García,
E. Urones-Garrote, D. Ávila-Brande,
R. Sáez-Puche,
J. P. Attfield* ______ **9340 – 9344**

Double Double Cation Order in the High-Pressure Perovskites $MnRMnSbO_6$

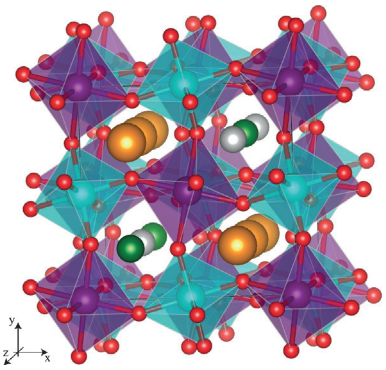

Cations called to order: A double double perovskite type structure is reported in the $MnRMnSbO_6$ compound series (R = La, Pr, Nd, Sm). The structure has Mn^{2+} and R^{3+} cations ordered in columns on perovskite A sites, while Mn^{2+} and Sb^{5+} ions have rock salt order on the B sites. The $MnRMnSbO_6$ double double perovskites are ferrimagnetic at low temperatures with additional spin-reorientation transitions.

Photoredox Reactions

S. M. Chen, Q. Q. Wan,
A. K. Badu-Tawiah* ______ **9345 – 9349**

Picomole-Scale Real-Time Photoreaction Screening: Discovery of the Visible-Light-Promoted Dehydrogenation of Tetrahydroquinolines under Ambient Conditions

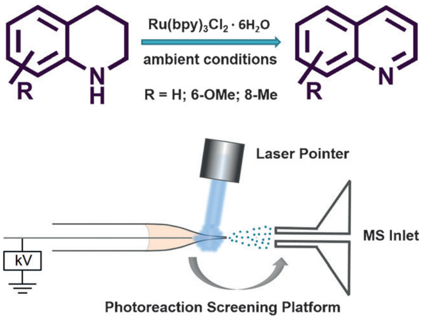

The here and now of it: A picomole-scale, real-time platform based on mass spectrometry for the screening of photoredox reactions enabled the discovery of an accelerated photocatalytic transformation of tetrahydroquinolines into quinolines under ambient conditions (see scheme). The screening platform also has the advantage that key mechanistic information can be derived from captured intermediates.

Protein Engineering

C. Giese, J. Eras, A. Kern, M. A. Schärer,
G. Capitani,
R. Glockshuber* ______ **9350 – 9355**

Accelerating the Association of the Most Stable Protein–Ligand Complex by More than Two Orders of Magnitude

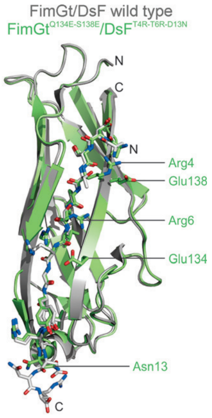

Accelerated binding of the protein FimGt to its natural peptide ligand DsF was achieved by rational design of FimGt and DsF variants with enhanced electrostatic interactions. Binding was accelerated by two orders of magnitude without structural perturbation of the complex. The most stable and fastest associating complex (see picture, shown in green) showed a dissociation constant of 8.8×10^{-22} M (wild-type complex shown in gray).

Capsid Self-Assembly

S. Milles, M. R. Jensen, G. Communie,
D. Maurin, G. Schoehn,
R. W. H. Ruigrok,*
M. Blackledge* ______ **9356 – 9360**

Self-Assembly of Measles Virus Nucleocapsid-like Particles: Kinetics and RNA Sequence Dependence

Inside Back Cover

Self-organization of the measles virus nucleoprotein into nucleocapsid-like particles was observed upon simple addition of RNA, allowing investigation of the nucleocapsid assembly process. Real-time NMR and fluorescence spectroscopy revealed biphasic assembly kinetics and demonstrate that assembly depends strongly on RNA sequence.

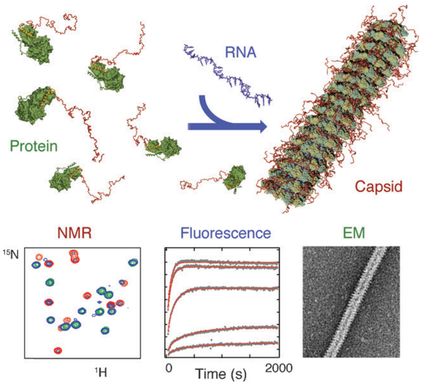

© 2016 Wiley-VCH Verlag GmbH & Co. KGaA, Weinheim

Enzyme Catalysis

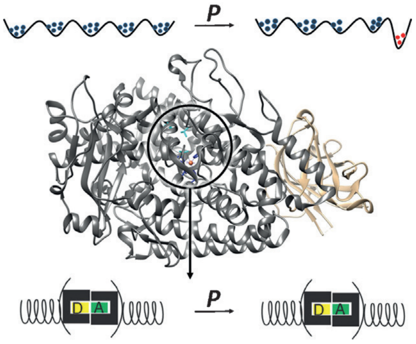

Under pressure: The effect of hydrostatic pressure (*P*) on the steady-state rate constants, substrate kinetic isotope effects, and the temperature dependency of these parameters enables isotope-dependent, local protein motions to be distinguished from the more global, isotope-independent conformational landscape in the primary C—H activation step of the enzyme soybean lipoxygenase-1 (structure shown, active site circled).

Imaging Techniques

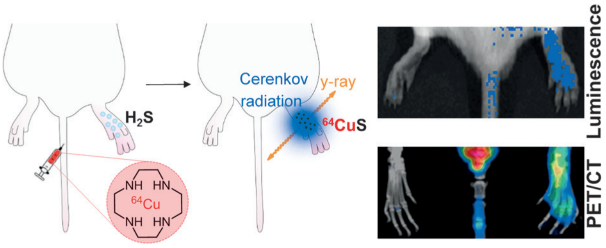

Pin it down: Radioactive copper probes were developed for the instant immobilization of the gas signaling molecule H_2S as solid ^{64}CuS, which was then quantified and visualized by optical and nuclear imaging (see picture). This highly sensitive and selective imaging technique is suitable for biomedical studies involving H_2S.

Polymerization

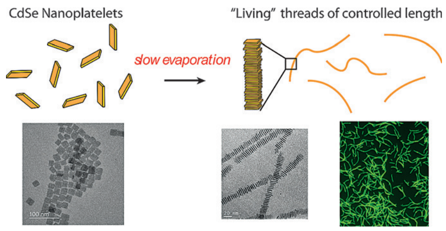

It's alive! A method to controllably assemble CdSe nanoplatelets into micron-long polymer-like threads is reported. Threads of a given length could be further grown through addition of supplementary nanoparticles, giving these structures living polymer characteristics.

Coordination Cages

The highest-nuclearity transition-metal–rare-earth heterometallic coordination cages $\{Ni_{64}RE_{96}\}$ (RE = Gd, Dy, and Y) with a cuboidal porous structure have been synthesized by using a mixed-ligand approach to control the hydrolysis of the metal ions. These giant cluster complexes exhibit high selectivity for CO_2 over CH_4 or N_2 at ambient temperature and a large magnetocaloric effect at ultralow temperatures.

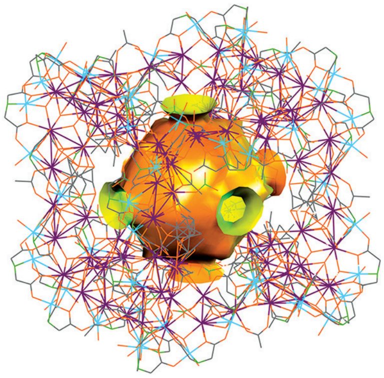

© 2016 Wiley-VCH Verlag GmbH & Co. KGaA, Weinheim

Antiperovskites

M. Valldor,* T. Wright, A. Fitch,
Yu. Prots ________ 9380 – 9383

Metal Vacancy Ordering in an Antiperovskite Resulting in Two Modifications of Fe_2SeO

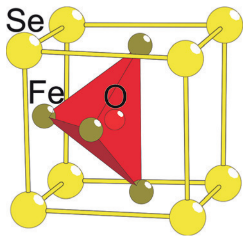

Two variants: Metal vacancy ordering in an antiperovskite results in two modifications of Fe_2SeO, which are pseudo-tetragonal and chiral, polar, non-centrosymmetric, and trigonal, respectively. Both modifications have similarities with ionic conductors. As the compounds seem to be insulating, the Fe is present as divalent high-spin ions because of weak crystal fields.

Carbocyclization

S. Zhou, J. Wang, L. Wang, C. Song,
K. Chen, J. Zhu* ________ 9384 – 9388

Enaminones as Synthons for a Directed C—H Functionalization: Rh^{III}-Catalyzed Synthesis of Naphthalenes

An easy way to carbocycles: Alkynes or α-diazo-β-ketoesters are the partners for enaminones in the Rh^{III}-catalyzed synthesis of the naphthalene framework, as shown in the picture. The installed aldehyde and hydroxy functional groups can be harnessed for further synthetic manipulation.

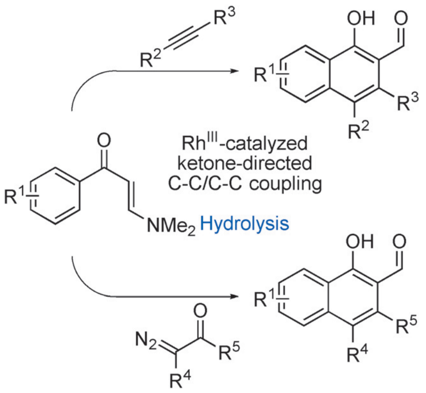

VIP

Hydrogen Production

J.-D. Xiao, Q. Shang, Y. Xiong, Q. Zhang,*
Y. Luo, S. H. Yu, H.-L. Jiang* 9389 – 9393

Boosting Photocatalytic Hydrogen Production of a Metal–Organic Framework Decorated with Platinum Nanoparticles: The Platinum Location Matters

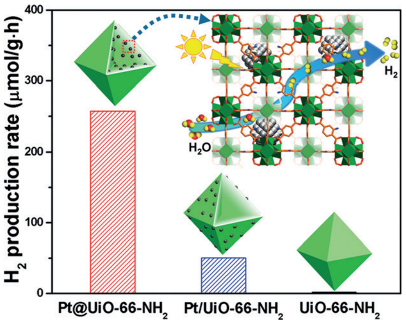

Location, location, location: Platinum nanoparticles (PtNPs) are incorporated inside or supported on a metal–organic framework (MOF), UiO-66-NH_2, giving Pt@UiO-66-NH_2 and Pt/UiO-66-NH_2, respectively. Having the Pt NPs inside the MOF greatly shortens the electron-transport distance, which favors the electron–hole separation and thereby yields the highest photocatalytic efficiency for H_2 production.

Magnetic Resonance Imaging

J. M. Bray, A. J. Davenport, K. S. Ryder,
M. M. Britton* ________ 9394 – 9397

Quantitative, In Situ Visualization of Metal-Ion Dissolution and Transport Using ^1H Magnetic Resonance Imaging

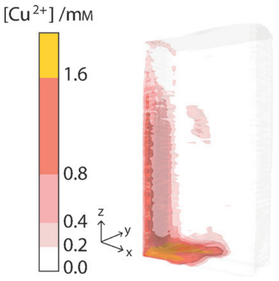

Insights into corrosion processes: Magnetic resonance imaging is used to quanitatively map the distribution of copper(II) ions during the electrodissolution of metallic copper (see picture). The method is non-invasive and can be applied in situ, in three dimensions, and in real time. The dissolution of Cu^{2+} ions is shown to be non-uniform across the anode.

© 2016 Wiley-VCH Verlag GmbH & Co. KGaA, Weinheim

Natural products: A chemo-enzymatic one-pot synthesis approach was developed for tricyclic microviridins comprising lactone as well as lactam rings. The method was used to design and screen protease-targeted libraries derived from short synthetic oligopeptides.

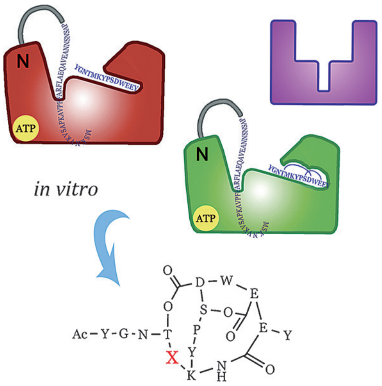

Biosynthesis

Re-cycling carbon dots: A recyclable ascorbate donor system coupled to clean two-electron phosphine oxidation circumvents the radical-mediated decomposition of molecular catalysts that limit sacrificial photocatalytic systems. When paired with a carbon quantum dot light absorber and DuBois-type nickel catalyst, the resultant hybrid photosystem sustained H_2 evolution for 5 days and reached a record $\mathrm{TON_{Ni}}$ of 1094 ± 61 in aqueous solution under AM1.5G solar irradiation.

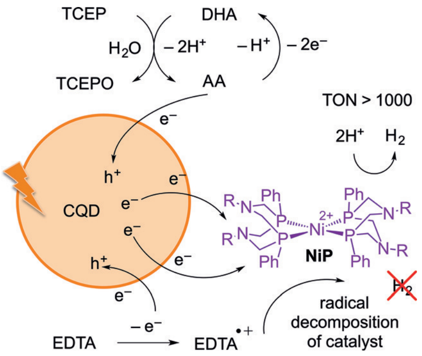

Carbon Dots

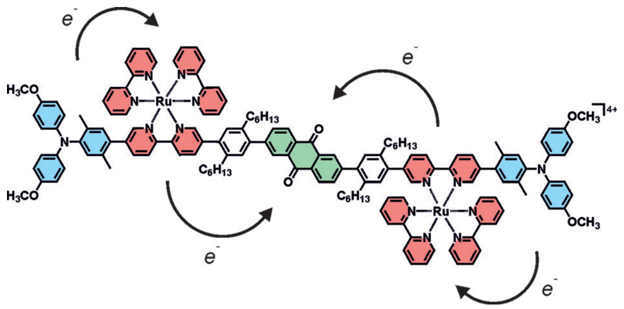

No sacrifice at all: Long-lived ($\tau = 870$ ns) electron accumulation has been achieved in a molecular pentad without the use of sacrificial reagents. This is an important proof-of-concept for solar-energy conversion and multi-electron photoredox chemistry.

Solar-Energy Conversion

Beta-Amyloid Aggregation

M. Amaro,* R. Šachl, G. Aydogan,
I. I. Mikhalyov, R. Vácha,
M. Hof* ________ **9411 – 9415**

GM$_1$ Ganglioside Inhibits β-Amyloid Oligomerization Induced by Sphingomyelin

Back Cover

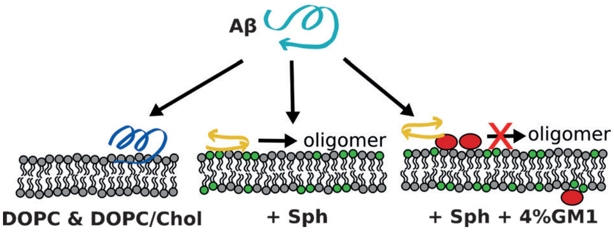

Fluorescence techniques show that sphingomyelin is a specific trigger for the spontaneous oligomerization of β-amyloid monomers and simulations suggest sphingomyelin induces the formation of β-sheet structures in monomeric peptides. Physiological amounts of GM$_1$ inhibit the oligomerization process, pointing to GM$_1$ as a protective factor rather than a booster of toxic oligomerization.

Radical Coupling

J. Xie, J. Yu, M. Rudolph, F. Rominger,
A. S. K. Hashmi* ________ **9416 – 9421**

Monofluoroalkenylation of Dimethylamino Compounds through Radical–Radical Cross-Coupling

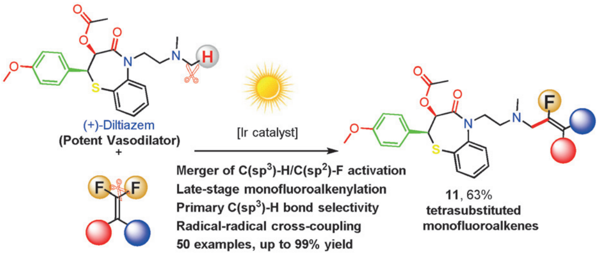

Privileged products: An α-C(sp^3)–H monofluoroalkenylation of unactivated tertiary amines through a mild, efficient, and redox-neutral route delivers privileged tetrasubstituted monofluoroalkenes under photoredox catalysis through the radical–radical cross-coupling of α-aminoalkyl radicals with monofluoroalkenyl radicals. This method enables the challenging late-stage monofluoroalkenylation of complex molecules.

Drug Design

M. Mondal, N. Radeva, H. Fanlo-Virgós,
S. Otto, G. Klebe,
A. K. H. Hirsch* ________ **9422 – 9426**

Fragment Linking and Optimization of Inhibitors of the Aspartic Protease Endothiapepsin: Fragment-Based Drug Design Facilitated by Dynamic Combinatorial Chemistry

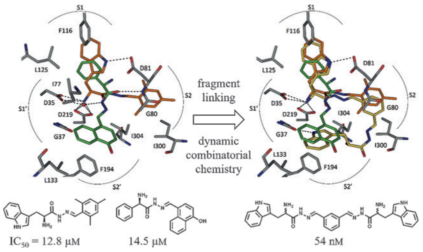

Better together: The synergistic combination of fragment linking and dynamic combinatorial chemistry represents a powerful and efficient strategy for accelerating hit identification and optimization, with the potential to afford new lead compounds. The most potent inhibitor of the aspartic protease endothiapepsin identified in this way exhibits an IC$_{50}$ value of 54 nM, which represents a 240-fold improvement in potency compared to the parent hits.

Algal Blooms

M. Scherer, D. Bezold,
K. Gademann* ________ **9427 – 9431**

Investigating the Toxicity of the Aeruginosin Chlorosulfopeptides by Chemical Synthesis

Toxic brew: Four chlorosulfopeptide congeners that are thought to be responsible for the adverse effects of algal blooms were prepared by chemical synthesis. The roles of the chloride and sulfate groups were then established by toxicity assays with the crustacean *Thamnocephalus platyurus*.

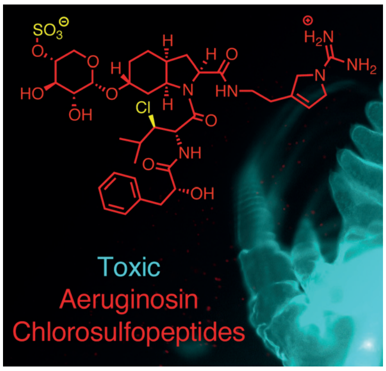

© 2016 Wiley-VCH Verlag GmbH & Co. KGaA, Weinheim

Carbon–Fluorine Bond Activation

J. Tanaka, S. Suzuki, E. Tokunaga,
G. Haufe, N. Shibata* ______ **9432 – 9436**

Asymmetric Desymmetrization via Metal-Free C–F Bond Activation: Synthesis of 3,5-Diaryl-5-fluoromethyloxazolidin-2-ones with Quaternary Carbon Centers

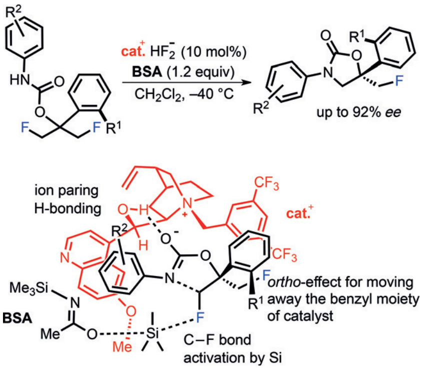

***ortho* Effect**: Non-activated C_{sp3}–F bonds can be cleaved selectively in the novel desymmetrization of 1,3-difluorides. The combination of a cinchona alkaloid based chiral ammonium bifluoride catalyst and *N*,*O*-bis(trimethylsilyl)acetamide facilitated the efficient, catalyzed asymmetric C_{sp3}–F bond cleavage. The steric *ortho* effect plays an important role in the asymmetric induction.

Pyrazolidin-3,5-diones

T. Gieshoff, D. Schollmeyer,
S. R. Waldvogel* ______ **9437 – 9440**

Access to Pyrazolidin-3,5-diones through Anodic N–N Bond Formation

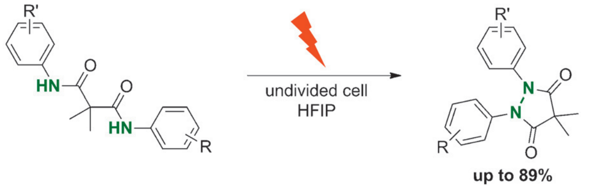

Tying up loose Ns: A novel synthetic approach to pharmacologically relevant heterocycles through anodic N–N bond generation was established. Readily accessible malonic dianilides provide an easy and efficient access to *N*,*N*′-diarylpyrazolidin-3,5-diones without the need for *N*,*N*′-diarylhydrazines as building blocks.

Supporting information is available on www.angewandte.org (see article for access details).

A video clip is available as Supporting Information on www.angewandte.org (see article for access details).

This article is available online free of charge (Open Access).

This article is accompanied by a cover picture (front or back cover, and inside or outside).

The Very Important Papers, marked VIP, have been rated unanimously as very important by the referees.

The Hot Papers are articles that the Editors have chosen on the basis of the referee reports to be of particular importance for an intensely studied area of research.

Check out these journals:

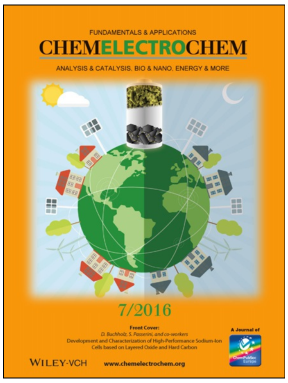
www.chemelectrochem.org

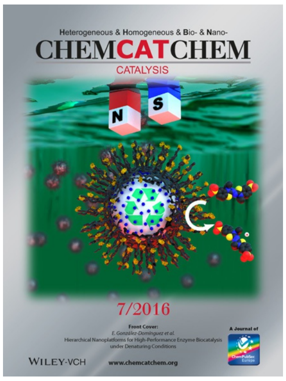
www.chemcatchem.org

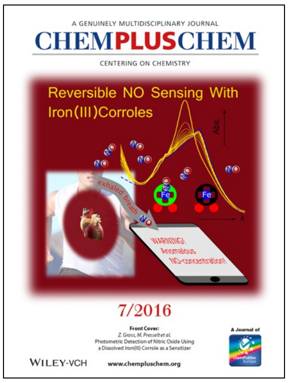
www.chempluschem.org

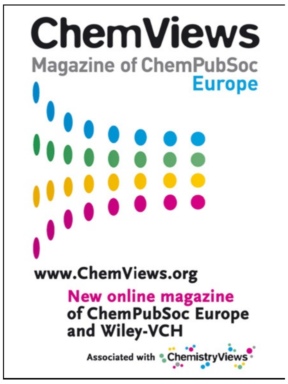

www.chemviews.org

© 2016 Wiley-VCH Verlag GmbH & Co. KGaA, Weinheim

Angewandte Corrigendum

An Unusually Small Singlet–Triplet Gap in a Quinoidal 1,6-Methano[10]annulene Resulting from Baird's 4*n* π-Electron Triplet Stabilization

B. C. Streifel, J. L. Zafra, G. L. Espejo,
C. J. Gómez-García, J. Casado,*
J. D. Tovar* ______________ **5888–5893**

Angew. Chem. Int. Ed. **2015**, *54*

DOI: 10.1002/anie.201500879

During their continued synthetic studies associated with the TMTQ quinoidal molecule reported in this Communication, the authors found that the NMR spectra of the new quinoidal derivatives were identical to those appearing in Figures S7 and S8 of the Supporting Information for this article. Due to the poor solubilities of TMTQ and related compounds, they realized that an impurity had been observed, now assigned as triphenylphosphine oxide based on comparisons to an authentic sample. This impurity presumably arises from oxidation of the ligands associated with the [Pd(PPh$_3$)$_4$] catalyst used for the Takahashi coupling.

A much purer sample of TMTQ has now been obtained using another Pd source and purification by repeated column chromatography. New spectra for Figures S7 and S8, along with an interpretation of the results, are available as a Supporting Information for this Corrigendum.

The UV-Vis-NIR absorption spectra and the IR and Raman spectra of the newly purified TMTQ were found to be identical to the original report, except for some expected differences in the fingerprint region of the IR spectrum (1000–700 cm^{-1}) that were not essential for the presented analysis. Therefore, the findings and interpretations of the initial report are not changed in any way.

The authors apologize for this oversight and they thank Prof. Michael M. Haley (University of Oregon) for raising some initial concerns about the VT-NMR data and sharing his own data.[1] Justin R. DeFrancisco (Johns Hopkins) determined and eliminated the source of the impurity and collected the new VT-NMR data.

---

[1] G. E. Rudebusch, J. L. Zafra, K. Jorner, K. Fukuda, J. L. Marshall, I. Arrechea-Marcos, G. L. Espejo, R. Ponce Ortiz, C. J. Gómez-García, L. N. Zakharov, M. Nakano, H. Ottosson, J. Casado, M. M. Haley, *Nature Chem.* **2016**, DOI: 10.1038/nchem.2518.

© 2016 Wiley-VCH Verlag GmbH & Co. KGaA, Weinheim